Eur J Nucl Med Mol Imaging (2018) 45:20–30
https://doi.org/10.1007/s00259-017-3850-x

ORIGINAL ARTICLE

Clinical performance of ^{68}Ga-PSMA-11 PET/MRI for the detection of recurrent prostate cancer following radical prostatectomy

Benedikt Kranzbühler[1] · Hannes Nagel[2] · Anton S. Becker[3] · Julian Müller[2] · Martin Huellner[2] · Paul Stolzmann[2] · Urs Muehlematter[2] · Matthias Guckenberger[4] · Philipp A. Kaufmann[2] · Daniel Eberli[1] · Irene A. Burger[2]

Received: 20 July 2017 / Accepted: 4 October 2017 / Published online: 14 October 2017

Abstract
Purpose Sensitive visualization of recurrent prostate cancer foci is a challenge in patients with early biochemical recurrence (EBR). The recently established ^{68}Ga-PSMA-11 PET/CT has significantly improved the detection rate with published values of up to 55% for patients with a serum PSA concentration between 0.2–0.5 ng/mL. The increased soft tissue contrast in the pelvis using simultaneous ^{68}Ga-PSMA-11 PET/MRI might further improve the detection rate in patients with EBR and low PSA values over PET/CT.
Methods We retrospectively analyzed a cohort of 56 consecutive patients who underwent a ^{68}Ga-PSMA-11 PET/MRI for biochemical recurrence in our institution between April and December 2016 with three readers. Median PSA level was 0.99 ng/mL (interquartile range: 3.1 ng/mL). Detection of PSMA-positive lesions within the prostate fossa, local and distant lymph nodes, bones, or visceral organs was recorded. Agreement among observers was evaluated with Fleiss's kappa (k).
Results Overall, in 44 of 56 patients (78.6%) PSMA-positive lesions were detected. In four of nine patients (44.4%) with a PSA < 0.2 ng/mL, suspicious lesions were detected (two pelvic and one paraaortic lymph nodes, and two bone metastases). In eight of 11 patients (72.7%) with a PSA between 0.2 and < 0.5 ng/mL, suspicious lesions were detected (two local recurrences, six lymph nodes, and one bone metastasis). Five out of 20 patients with a PSA < 0.5 ng/mL had extrapelvic disease. In 12 of 15 patients (80.0%) with a PSA between 0.5 and < 2.0 ng/mL, suspicious lesions were detected (four local recurrences, nine lymph nodes, and four bone metastases). In 20 of 21 patients (95.2%) with a PSA >2.0 ng/mL, suspicious lesions were detected. The overall interreader agreement for cancer detection was excellent (κ = 0.796, CI 0.645–0.947).
Conclusions Our data show that ^{68}Ga-PSMA-11 PET/MRI has a high detection rate for recurrent prostate cancer even at very low PSA levels <0.5 ng/mL. Furthermore, even at those low levels extrapelvic disease can be localized in 25% of the cases and local recurrence alone is seen only in 10%.

Keywords Prostate cancer · Prostate-specific antigen · ^{68}Ga-PSMA-11 · Positron emission tomography · PSMA antigen

Electronic supplementary material The online version of this article (https://doi.org/10.1007/s00259-017-3850-x) contains supplementary material, which is available to authorized users.

✉ Irene A. Burger
Irene.burger@usz.ch

[1] Department of Urology, University Hospital Zürich, University of Zürich, Zürich, Switzerland

[2] Department of Nuclear Medicine, University Hospital Zürich, University of Zürich, Rämistrasse 100, 8091 Zürich, Switzerland

[3] Department of Radiology, University Hospital Zürich, University of Zürich, Zürich, Switzerland

[4] Department of Radiation Oncology, University Hospital Zürich, University of Zürich, Zürich, Switzerland

Introduction

Despite substantial improvements in early detection and local treatment, prostate cancer still represents the third leading cause of cancer-related death in men after lung and colorectal cancer [1]. Depending on the individual risk category, the disease will recur in about 20% to 40% of all patients after initial curative treatment (radical prostatectomy or external beam radiation therapy) [2–5]. Following radical

prostatectomy, biochemical recurrence is defined as two confirmed prostate specific antigen (PSA) values >0.2 ng/mL [6]. Salvage radiotherapy (sRT) is currently the treatment of choice for patients with early biochemical recurrence (EBR) after radical prostatectomy. Recent studies demonstrated improved efficacy when sRT was performed at PSA values <0.2 ng/mL [7–9]. However, in up to 30% of patients, sRT does not affect PSA levels, most likely due to extrapelvic localization of the recurrence [10]. Therefore, an imaging modality detecting the tumor localization in EBR even at very low PSA values would be desirable. So far, multiparametric magnetic resonance imaging (mpMRI) or choline positron emission tomography/computerized tomography (PET/CT) were most commonly used for recurrence detection in prostate cancer. Recently published data for combined whole body MRI with dedicated pelvic mpMRI showed an overall detection rate of 21% in patients with PSA levels between 0.05–56.12 ng/mL (median 0.36 ng/mL) [11]. Also the sensitivity of choline PET/CT is low in patients with PSA levels <1 ng/mL, with a mean detection rate of 20% [12, 13]. Therefore, a differentiation between local recurrence and oligometastatic disease in patients with EBR was almost impossible and inhibited a precise stratification to appropriate treatment modalities.

The ^{68}Gallium labeled tracer targeting the prostate specific membrane antigen (PSMA) ^{68}Ga-PSMA-11 used in combined PET/CT has significantly improved the tumor detection rate in patients with EBR, being as high as 55% in patients with a PSA of 0.2–0.5 ng/mL [14–16]. Its efficacy has also been shown in patients after primary external beam radiation therapy [17]. However, the proximity of the bladder to the prostate fossa still impairs the detection of local recurrence in the prostate bed. Increased soft tissue contrast in the pelvis using PET/MRI instead of PET/CT might further improve the detection rate for patients with EBR [18, 19]. Improved tumor localization in the initial staging has already been shown for ^{68}Ga-PSMA-11 PET/MRI [20]. However, a drawback in pelvic PET/MRI is the fact that on commercially available systems bone information is not yet available for attenuation correction (AC). This is substantially affecting the accuracy of PET images within or close to bony structures, since the missing density in the MRI based AC map will lead to an underestimation of the PET activity [21]. Recently, it was shown, that the integration of time-of-flight (TOF) information can significantly reduce image artifacts due to metal implants or bony structures and improve image quality in simultaneous PET/MRI [22, 23]. Therefore, further improvements in the detection rate of patients with very low PSA values at scan might be expected using a PET/MRI with TOF capability for image analysis.

We retrospectively evaluated ^{68}Ga-PSMA-11 TOF-PET/MRI in our single center cohort with regard to lesion detection rate in patients with biochemical recurrence after prostatectomy.

Patients and methods

Patients

This retrospective study included all patients who underwent ^{68}Ga-PSMA-11 PET/MRI for biochemical recurrence after prostatectomy at the Department of Nuclear Medicine (UniversityHospital Zürich) between April and December 2016. The local ethics committee approved the study protocol and all patients gave a general written informed consent for retrospective use of their data (BASEC Nr. 2016–02230). Recorded patient characteristics included age at scan, preoperative prostate specific antigen (PSA) value and PSA value at scan. Additionally, initial tumor stage/ grade and Gleason score as well as the postoperative resection margin status (R0 vs. R1) and prior androgen-deprivation therapy (ADT) were assessed. We analyzed the detection of PSMA-positive lesions overall and according to the region of detection: prostate fossa, local and distant lymph nodes, bone lesions and visceral lesions. Lymph node regions were further divided into 1) pelvic, 2) para-aortic, 3) mediastinal/supraclavicular, and 4) axillary. Furthermore, the maximum standardized uptake value (SUV_{max}) and the applied amount of tracer were analyzed.

^{68}Ga-PSMA-11 PET/MRI

All patients underwent a single injection of ^{68}Ga-PSMA-11 (mean dose ± standard deviation, 123.34 ± 16.1 MBq, range 90–153 MBq). A clinical routine whole-body PET/MRI was performed 60 min after injection on a hybrid scanner (SIGNA PET/MR, GE Healthcare, Waukesha, WI, USA) used in previous studies at our department [24]. The scanner comprises a 3-T MR system with TOF-PET detector ring installed between the body and gradient coils. A whole-body MR localizer scan was started before acquisition of PET data. Subsequently a 3D dual-echo, spoiled gradient recalled echo sequence (LAVA-FLEX) for AC, and a PET emission scan was recorded in list mode. The default number of bed positions was six and the acquisition time per bed position was 2 min. The whole-body protocol furthermore included specific sequences covering the pelvis, including a high resolution T1-weighted LAVA-FLEX sequence, T2-weighted fast recovery fast spin-echo sequence in two planes and diffusion weighted images (b values: 0, 300, 1000). To reduce ^{68}Ga-PSMA-11 activity in the bladder, ureters, and kidneys, furosemide was injected intravenously 30 min prior to the ^{68}Ga-PSMA-11 injection (0.13 mg/kg), and patients were asked to void prior to the scan. For attenuation correction an atlas-based MR-AC was used for the head, and for the remaining body air, lung, and soft tissue were segmented using the DIXON LAVA-FLEX sequences generating a fat-water based attenuation correction map. Details regarding the MRI sequences are given in the supplements (Supplement Table 1).

The protocol scan time was 30 min. A dual board-certified radiologist and nuclear medicine physician (R1), incorporating both the MRI and PET information, analyzed all images. To investigate the influence of the different imaging modalities additional readouts including only MRI sequences (MRI_{only}) and ^{68}Ga-PSMA-11 PET with only water weighted axial DIXON LAVA-FLEX (PET_{only}) were performed. Furthermore, to analyze interreader variability 2 additional readouts by radiologist with 2 (R2) and 0.5 years (R3) of nuclear medicine experience were conducted. The readers extracted clinical information for every readout. For the PET/MRI readout only lesions with high suspicion for recurrence were considered positive: focal ^{68}Ga-PSMA-11 uptake in the soft tissue of the prostate bed, lymph nodes with an $SUV_{max} \geq 3$ and/or pathologically increased size (≥ 5 mm for perirectal nodes, ≥ 8 mm for iliac / retroperitoneal nodes, ≥ 1 cm for inguinal nodes), focal bone uptake with correlating bone marrow replacement or focal uptake with correlating soft tissue lesion.

Statistical analysis

Descriptive statistics were used to display patient data as median, interquartile range (IQR), or number (percent). The detection rate was plotted against the absolute prostate specific antigen (PSA) value in ng/mL at scan. Images were generated using GraphPad Prism version 7 (PraphPad Software, Inc. La Jolla, CA, USA). Agreement among observers was evaluated with R (v. 3.4.0. R Foundation for Statistical Computing, Vienna, Austria; package DescTools v. 0.99.20) using Fleiss's kappa (κ) [25] for all readers and Cohen's κ for each reader pair [26]. Ninety-five percent confidence intervals (CIs) are reported for κ values. Interpretation of κ and ICC was based on a classification provided by Landis and Koch: 0.0, poor; 0.0–0.20, slight; 0.21–0.40, fair; 0.41–0.60, moderate; 0.61–0.80, good; 0.81–1.00, almost-perfect reproducibility [27].

Results

A total of 56 patients were retrospectively analyzed. Patient characteristics are shown in Table 1. Median age at scan was 69 years (IQR: 11), and median preoperative PSA value was 9.3 ng/mL (IQR: 12.7). All patients underwent initial radical prostatectomy. Twenty-five patients (44.6%) presented with an initial tumor stage pT2. Twenty-six patients (46.4%) had a pT3 tumor and 1 patient (1.8%) had a pT4 tumor. The median Gleason score was 7 (IQR: 2). Twenty-three percent of all included patients were initially nodal positive (N1), primary metastatic disease (M1) was not reported in any patient. A postoperative positive resection margin was reported in 26 patients (46.4%). Non-imaging guided salvage radiotherapy of the prostate bed was performed in 27 patients (48.2%).

Table 1 Patient characteristics

Characteristics	*n* = 56
Age (years)	69 (11)
Initial PSA (ng/mL)	9.3 (12.7)
PSA at scan (ng/mL)	0.99 (3.1)
Stage (n)	
pT2	2 (3.6%)
pT2a	1 (1.8%)
pT2b	4 (7.1%)
pT2c	18 (32.2%)
pT3	2 (3.6%)
pT3a	11 (19.6%)
pT3b	13 (23.2%)
pT4	1 (1.8%)
N/A	4 (7.1%)
N positive	13 (23.2%)
M positive	0
Gleason score (n)	
6	5 (8.9%)
7	25 (44.7%)
8	6 (10.7%)
9	13 (23.2%)
N/A	7 (12.5%)
R1 resection (n)	26 (46.4%)
Previous ADT (n)	8 (14.2%)

Data presented as median (interquartile range) or number (percent)

Pre-scanning ADT was administered in 8 patients (14.2%). Seven of these patients had intermittent ADT several years before the scan. Only 1 patient had continuous ADT at the time of the ^{68}Ga-PSMA-11 PET/MRI. The total scan time per patient ranged from 25 to 57 min, with a median scan time of 42 min.

The ^{68}Ga-PSMA-11 PET/MRI, the MRI_{only} and the PET_{only} findings of all 56 patients listed by increasing PSA values at scan are displayed in Table 2. In two patients, MRI_{only} was not evaluated, since the protocol was not complete. Overall, in 44 of 56 patients (78.6%) PSMA-positive lesions were detected using ^{68}Ga-PSMA-11 PET/MRI. Detection rates subdivided by the PSA value at scan and the location of recurrence are shown in Fig. 1.

The detection rate of MRI_{only} was significantly lower compared to PET/MRI with 13 of 54 patients (24%). The overall detection rate of PET_{only} was comparable with PET/MRI with 43 of 56 patients (76%). However, six lesions suspicious on PET_{only} were interpreted as physiologic activity on PET/MRI and 6 suspicious lesions on PET/MRI were missed on PET_{only}. MRI_{only} was significantly inferior to PET/MRI and PET_{only} especially for the detection of lymph node and bone metastases (Supplement Table 2).

Table 2 Detection pattern by ^{68}Ga-PSMA-11 PET/MRI (MRI_{only} / PET_{only})

Nr.	PSA at scan (ng/ml)	LR PET/MRI (MRI / PET)	SUV_{max}	LM PET/MRI (MRI / PET)	SUV_{max}	LN size (mm)	LN location	BM PET/MRI (MRI / PET)	SUV_{max}	Dosage (MBq)
1	0.05	- (-/-)		- (-/-)				- (-/-)		107
2	0.08	- (-/-)		- (-/-)				- (-/-)		114
3*	0.08	- (-/-)		+ (+/+)	17.1	5	2	- (-/-)		90
4	0.09	- (-/-)		+ (-/+)	4.8	8	1	+ (-/-)	3.8	146
5	0.12	- (-/-)		- (-/-)				- (-/-)		120
6	0.13	- (-/-)		- (-/-)				- (-/-)		150
7	0.14	- (-/-)		- (-/-)				+ (-/+)	4.1	113
8	0.15	- (-/-)		+ (-/+)	15	8	1	- (-/-)		126
9	0.17	- (-/-)		- (-/-)				- (-/-)		102
10	0.2	- (-/-)		+ (-/+)	4.1	10	2,1	- (-/-)		143
11	0.21	- (-/+)		+ (-/+)	18	4	1	- (-/-)		121
12	0.22	- (-/+)		+ (-/+)	6.4	3	1	- (-/-)		101
13	0.26	- (-/-)		- (-/-)				- (-/-)		135
14	0.27	- (-/-)		+ (+/+)	3.7	4	1	- (-/-)		145
15	0.31	- (-/-)		+ (-/+)	4.9	4	1	- (-/-)		107
16	0.33	- (-/-)		- (-/+)				- (-/-)		136
17	0.35	- (na/-)		- (na/-)				+ (na/+)	16.3	121
18	0.36	- (-/+)		- (+/-)				- (-/-)		128
19	0.45	+ (-/+)	13.7	- (-/+)				- (-/-)		137
20	0.49	+ (-/+)	4.4	- (+/+)				- (-/-)		143
21	0.51	+ (-/+)	13	- (-/-)				- (-/-)		105
22	0.6	- (-/-)		+ (-/+)	4.9	4	1	- (-/-)		103
23	0.6	- (-/-)		- (-/-)				- (-/-)		108
24	0.67	- (+/-)		- (-/-)				+ (-/+)	3.9	147
25	0.68	- (-/-)		+ (-/+)	6.1	3	1	- (-/-)		111
26	0.71	+ (na/-)	8.3	+ (na/+)	4.1	1.7	1	- (na/-)		110
27	0.8	- (-/-)		+ (-/+)	11.9	12	1	+ (+/+)	12.9	111
28	0.96	- (-/-)		+ (-/+)	3.7	3	1	+ (-/+)	5.9	105
29	1.02	- (-/-)		+ (-/+)	11.6	6	1	- (-/-)		109
30	1.04	- (-/-)		+ (-/-)	6.1	7	1	- (-/-)		127
31	1.05	+ (-/+)	9.8	- (-/-)				- (-/-)		141
32	1.16	- (-/-)		- (-/-)				- (-/-)		106
33	1.45	- (-/-)		- (-/-)				- (-/+)		149
34	1.8	- (-/-)		+ (-/+)	15.6	5	1,2	+ (-/+)	10.7	123
35	1.8	+ (+/+)	18.1	- (-/-)				- (-/-)		135
36	2.04	- (-/-)		+ (-/+)	40.7	5	1	- (-/-)		105
37	2.09	- (-/-)		+ (+/-)	2.6	8	1	- (-/-)		147
38	2.2	+ (-/+)	9.1	+ (-/+)	9.7	8	1	- (-/-)		139
39	2.22	- (-/-)		+ (-/+)	47	16	1,2,3	- (-/-)		134
40	2.5	- (-/-)		+ (-/+)	5.7	5	1	- (-/-)		107
41	2.74	- (-/-)		+ (-/+)	12	3	1,2,3	- (-/-)		137
42	3	- (-/-)		+ (-/+)	7.5	4	2,1	+ (-/+)	27.2	112
43	3.5	- (-/-)		+ (-/+)	8.8	6	1	- (-/-)		107
44	4	- (-/-)		+ (-/+)	20.3	9	2,1,3	- (-/-)		107
45	4.1	+ (+/+)	19.7	- (-/-)				- (-/-)		133
46	4.2	- (-/-)		+ (+/+)	14.2	6	1	- (-/-)		134
47	4.29	- (-/-)		+ (-/-)	8.8	6	2	- (-/-)		150
48	4.5	+ (-/+)	18.7	- (-/-)				- (-/-)		115
49	4.65	- (-/-)		- (-/-)				- (-/-)		128
50	5.4	- (-/-)		+ (-/+)	36	8	2,1	+ (-/+)	19.8	141
51	7.6	+ (+/+)	15.3	- (-/-)				- (-/-)		131
52	8.45	- (-/+)		+ (-/+)	7.3	8	1,4	+ (-/+)	24	125
53	9.4	- (-/-)		+ (-/+)	10.2	6	1	- (-/-)		152
54	18.6	- (-/-)		+ (-/+)	128	15	1,2	- (-/-)		123
55	20.03	- (-/-)		+ (-/+)	24	7	3,2,1	+ (-/+)	19.5	106
56†	30	- (-/-)		- (-/-)				- (-/-)		118

The detection based on R1 for PET/MRI is given, as well as the detection on MRI_{only} and PET_{only} in brackets

Patients with suspicious findings on ^{68} Ga-PSMA-11-PET/MR are highlighted gray; patients without suspicious finding are white

PSA: Prostate Specific Antigen, LR: Local recurrence, LM: Lymph node metastasis, LN: Lymph node, BM: Bone metastasis, SUV_{max}: Maximum Standardized Uptake Value

LN location: 1 = pelvic, 2 = paraaortal, 3 = mediastinal/supraclavicular, 4 = axillary.

*Patient with androgen deprivation therapy at the time of scan

†Patient with peritoneal carcinomatosis

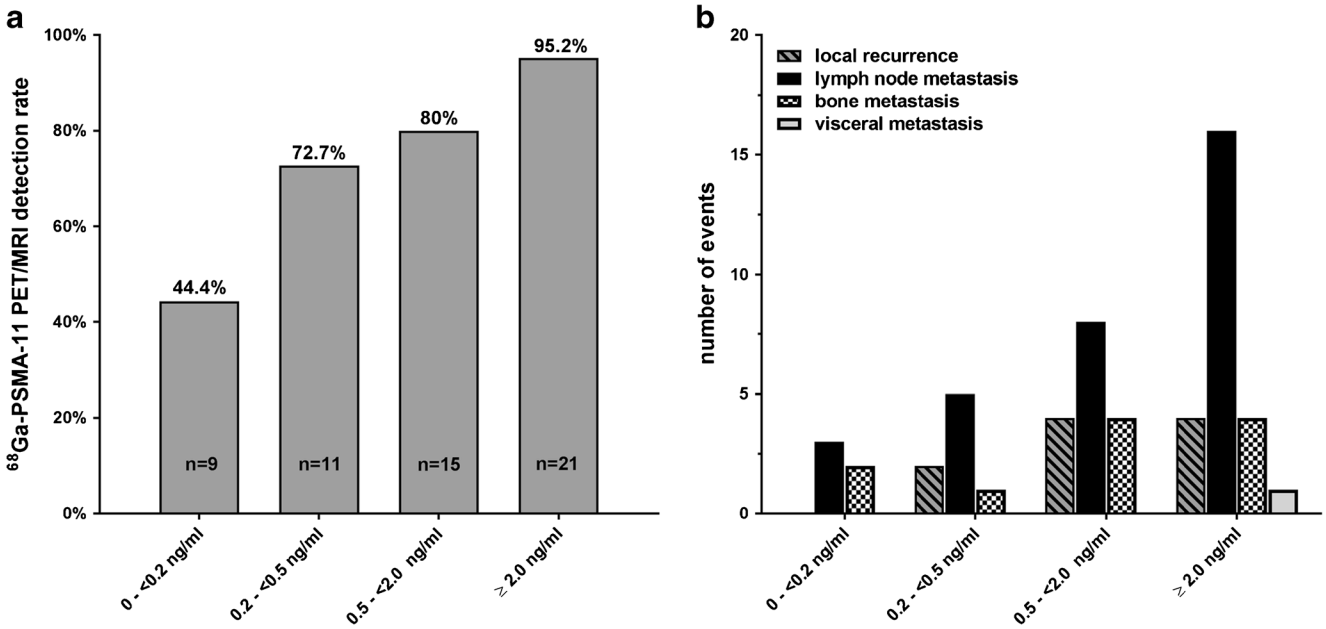

Fig. 1 Detection rate by ^{68}Ga-PSMA-11 PET/MRI. **a** ^{68}Ga-PSMA-11 PET/MRI detection rate stratified by different PSA levels at time of scan. **b** Number of ^{68}Ga-PSMA-11 PET/MRI positive events stratified by side and PSA levels at time of scan

The detection rate was 44% (four of nine patients) for PSA values of 0 to < 0.2 ng/mL. Suspicious lesions were detected in pelvic (n = 2) and para-aortic (n = 1) lymph nodes and in the bone (scapula, sternum, n = 2). In patients with a PSA between 0.2 and < 0.5 ng/mL, the detection efficacy increased up to 72.7% (eight of 11 patients). Positive lesions were detected in the prostate fossa (local recurrence; n = 2), in pelvic (n = 5), and para-aortic (n = 1) lymph nodes and in the sacrum (n = 1). In 12 of 15 (80%) patients with a PSA between 0.5 and < 2.0 ng/mL, suspicious lesions were detected. Sites of detection were the prostate fossa (local recurrences; n = 4), pelvic (n = 8), and para-aortic (n = 1) lymph nodes, as well as bone metastases in four patients. In 20 of 21 patients (95.2%) with a PSA >2.0 ng/mL at scan, at least one lesion was PSMA-positive. Three of these patients presented only local recurrence at scan time (PSA 4.1, 4.5, and 7.6 ng/mL); one patient demonstrated additional PSMA-positive pelvic lymph nodes (PSA 2.2 ng/mL). Lymph node metastases were found in 16 of these patients: seven patients presented pelvic lymph nodes only, three patients presented pelvic and para-aortic lymph nodes, four patients presented pelvic, para-aortic and mediastinal/supraclavicular lymph nodes, one patient presented pelvic and axillary lymph nodes. In four patients, additional bone metastases were found. Bone marrow abnormalities were detected in all sites of suspicious PSMA uptake (Supplement Figure 1).

One patient presented with a single PSMA-positive lesion within the liver (PSA 30 ng/mL). Subsequently performed liver MRI confirmed a lesion of the falciform ligament that was further investigated with laparoscopy and histologically confirmed as peritoneal carcinomatosis. Interestingly, one patient with a PSA of 4.65 ng/mL at scan time was completely PSMA-negative. Re-imaging was performed using ^{18}F–Choline PET/CT to overcome a possible PSMA-negative tumor. However, also ^{18}F–Choline PET/CT could not reveal any metastatic lesion. Exemplary images of local recurrence, lymph node and bone metastases are shown in Figs. 2, 3, 4, and 5.

Median SUV_{max} was 11.4 (IQR: 8.5) in local recurrence and 9.4 (IQR: 16) in bone metastases. In PSMA-positive lymph nodes a median SUV_{max} of 9.7 (IQR: 12.3) corresponded to a median node size of 6 mm (IQR: 4).

The overall interreader agreement for the three readers for cancer detection was excellent (kappa = 0.796, CI 0.645–0.947), with almost perfect agreement for bone metastasis (kappa 0.924), and substantial agreement for lymph node metastasis (kappa = 0.697, CI 0.556–0.838) and local recurrence (kappa = 0.66, CI 0.522–0.808). The pairwise interreader agreement is given in the Supplement Table 3, showing an almost perfect agreement between R1 and R2.

Discussion

In our current patient population ^{68}Ga-PSMA-11 PET/MRI revealed a high overall detection rate of 78.6% in patients with biochemical recurrence after radical prostatectomy. The detection rate was only slightly lower for PSA values between 0.2 and < 0.5 ng/mL at scan. These results underline the promising potential of ^{68}Ga-PSMA-11 PET/MRI as re-staging tool

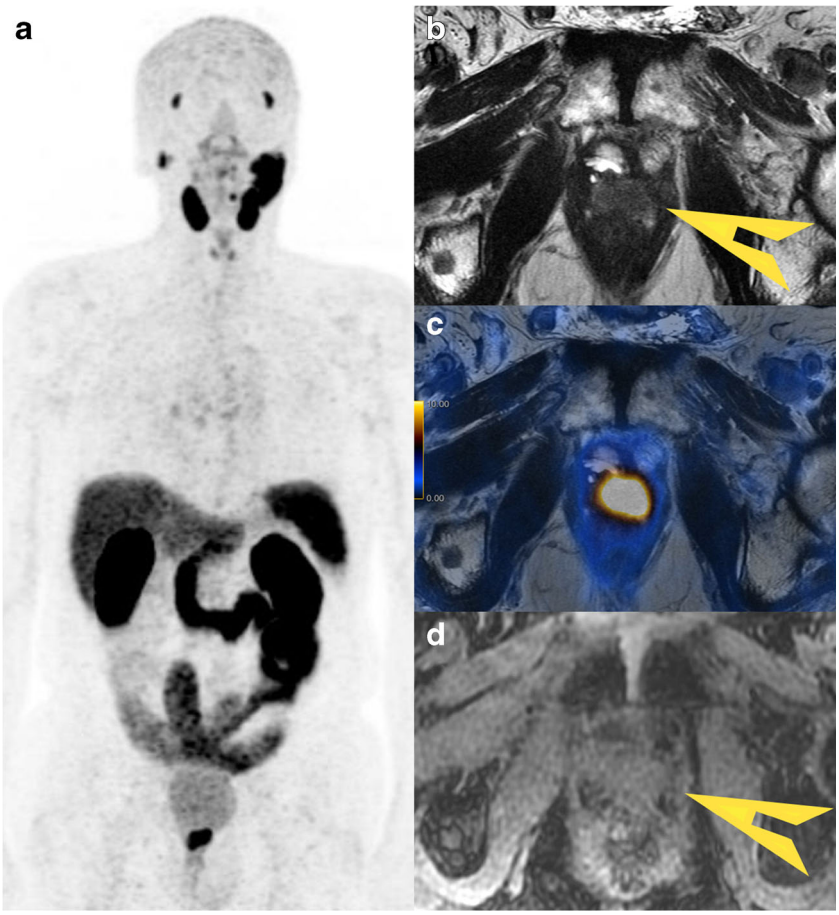

Fig. 2 Local recurrence in ^{68}Ga-PSMA-11 PET/MRI. **a** MIP ^{68}Ga-PSMA-11 PET of a eighty-four year old patient with a single PET/MRI positive lesion of 1.4 × 2.0 × 2.3 cm, SUV_{max} 19.7 between bladder neck and rectum (PSA 4.1 ng/ml). Radical prostatectomy had been performed 18 years ago. Initial tumor stage was pT2b, pN0 (0/9), cM0, G2, Gleason 3 + 3 = 6, R1. No signs of lymph node or bone metastases were detectable. **b** axial T2 weighted image shows obvious soft tissue lesion (arrow), with good correlation to the increased ^{68}Ga-PSMA-11 uptake on fused PET/MR images **c)**. **d** The lesion can be seen also on the axial water weighted DIXON LAVA-FLEX sequence

for prostate cancer patients with early biochemical recurrence and low PSA values.

A direct comparison of our overall detection rate to other reports in the literature is difficult owing to the low number of series combining ^{68}Ga-PSMA-11 PET with MRI and owing to different patient characteristics at the time of scan [18, 19, 28]. Afshar-Oromieh et al. reported a comparable overall detection rate of 80% in their initial experience including 20 consecutive patients [18]. However, the median PSA value at scan in their cohort was considerably higher, with 2.62 ng/mL (range of 0.51–73.60 ng/mL) compared to a median PSA of 0.99 ng/mL (range of 0.05–30 ng/mL) in our cohort. A study including 119 patients undergoing simultaneous ^{68}Ga-PSMA-11 PET/MRI and PET/CT showed an overall PSMA-positive rate of 78.2% [19], again with a higher median PSA value of 1.7 ng/mL (confidence interval: 1.25–2.2) at scan. The same group reported a similar accuracy in detecting lymph node and bone metastases using a non-TOF ^{68}Ga-PSMA-11 PET/MRI compared to PET/CT [28]. The largest series of patients published so far by Afsahr-Oromieh et al. including 1007 patients had an overall detection rate of 79.5% with a median PSA of 2.2 (range 0.01–1′ 237 ng/mL) [29].

The detection rate was significantly lower for the MRI_{only} readout in our cohort (24%), which is in line with first results from Robertson et al. (21%) [11]. However, the present protocol is not a clinically acceptable whole body MRI, with high resolution images in only one plane, and no whole body DWI. Therefore, we would like to emphasize that our results of the MRI_{only} readout probably underestimate the potential of whole body MRI and were only performed to gauge the information-gain from the added PSMA-PET. Only one lesion was rated suspicious on MRI_{only} and negative on PET/MRI or PET_{only}. After interpretation of the MRI images with the PET the lesion was interpreted rather as scar tissue by R2. PET_{only} had a superior detection rate compared to MRI_{only} with only six false negative and eight false positive lesions.

The interreader agreement between R1 and R2 was almost perfect and good between R1 and R3. R3 has only a limited experience with nuclear medicine readouts. These results are in line with the interobserver assessments by Fendler et al. for ^{68}Ga-PSMA PET/CT and suggest that the interpretation of PET/MRI is as robust as the interpretation of PET/CT [30].

The most challenging and clinically important cohort are patients with PSA values <0.5 ng/mL at the time of scan. These patients might benefit from a targeted salvage

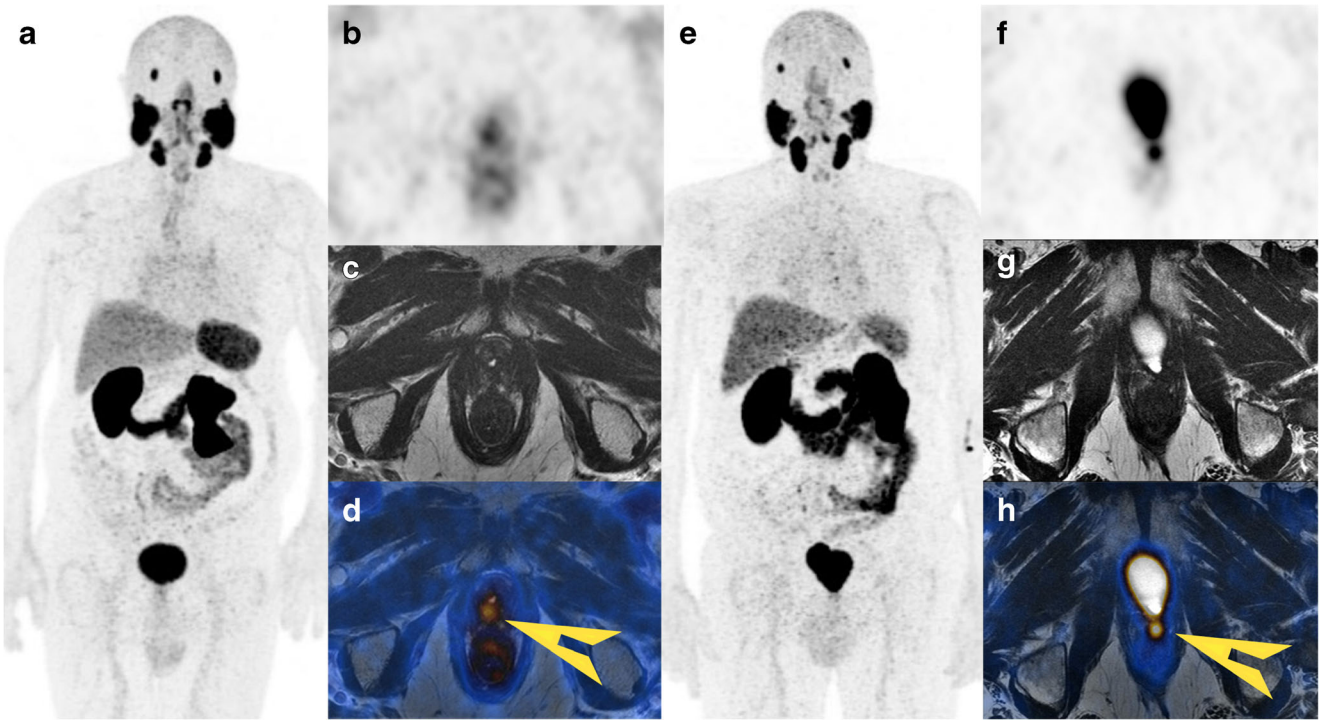

Fig. 3 Small PSMA-positive local recurrences in low PSA values (~0.5 ng/mL). **a** MIP ^{68}Ga-PSMA-11 PET of a 71-year-old patient with a PSA level of 0.49 ng/mL at scan time. **b** Unclear uptake on axial ^{68}Ga-PSMA-11 PET. **c** No suspicious focus on T2 axial imaging, **d** however clear projection of small focal PET-positive lesion (SUV_{max}: 4.4) in the right dorso-lateral prostate fossa (arrow), suspicious for local recurrence. **e** MIP ^{68}Ga-PSMA-11 PET of a 74-year-old patient (PSA 0.51 ng/mL at scan) with initial pT2c, pN0, M0, Gleason score 3 + 3 = 6. Similar findings of **f** unlear ^{68}Ga-PSMA-11 uptake, **g** no suspicious finding on anatomical imaging, however **h** clear projection of PET-positive lesion (SUV_{max}: 13) into the soft tissue, indicating local tumor recurrence

radiotherapy or local surgery of oligo-metastatic disease at the site of recurrence [7, 31]. In our cohort, 25% of the PSMA-positive recurrences in patients with PSA values <0.5 ng/mL were located outside the pelvis. Local recurrence alone was seen only in 10% of patients in this subgroup, while 35% of patients presented with pelvic lymph node metastases and 15% with bone metastases. Therefore, most of these patients probably would not benefit from a non-targeted salvage radiotherapy to the prostate fossa alone, which is, in the absence of imaging-detected metastases, still standard of care in patients with EBR following radical prostatectomy [3].

The detection rate in our cohort was 72.7% in patients with low PSA values between 0.2 and <0.5 ng/mL. The hitherto highest reported detection rates in patients with the same PSA range using ^{68}Ga-PSMA-11 PET/CT by two different groups were 57.9% and 50% [14, 15, 29], respectively. Furthermore, a detection rate of 44% has been reported in 27 patients with a PSA <1 ng/mL, and of 50% in 22 patients with PSA values between 0.2 and 2 ng/mL [32, 33]. The largest cohort published had a detection rate of 46% in 108 patients with PSA values between 0.2 and < 0.5 ng/mL [29]. However, the patient number in most of the aforementioned studies and in our own cohort are rather low, making it difficult to draw a definitive conclusion.

Our data show a local recurrence in 17.8% (10/56) of the patients. However, only two of these patients had a PSA <0.5 ng/mL at scan. Five patients with a PSA <0.5 ng/mL presented a PSMA-positive extra pelvic focus. Other groups reported a local recurrence in 35.1% (n = 248), 15.1% (n = 119), 21.6% (n = 37), and 0% (n = 20) of their patients [15, 18, 19, 34].

PSMA-positive lymph nodes were detected in 57.1% of our patients, whereas bone lesions were detected in 19.6%.These data are comparable to the collective of Eiber et al., who reported PSMA-positive lymph nodes in 57.6% and bone lesions in 35.9% [15]. An association between rising PSA values and PSMA-positive lymph nodes is not surprising. Yet, the three PSMA-positive bone lesions in patients with a PSA <0.5 ng/mL have to be highlighted, since bone lesions are usually not expected in patients with such low PSA values.

^{68}Ga-PSMA-11 is almost completely excreted renally and several studies demonstrated a significant halo-effect impairing the image quality around the kidneys and the bladder [35–37]. Most centers use a 60 min interval between tracer injection and image acquisition [37–40]. Attempts to reduce artifacts due to high tracer accumulation in the bladder and the kidneys include wash-out of

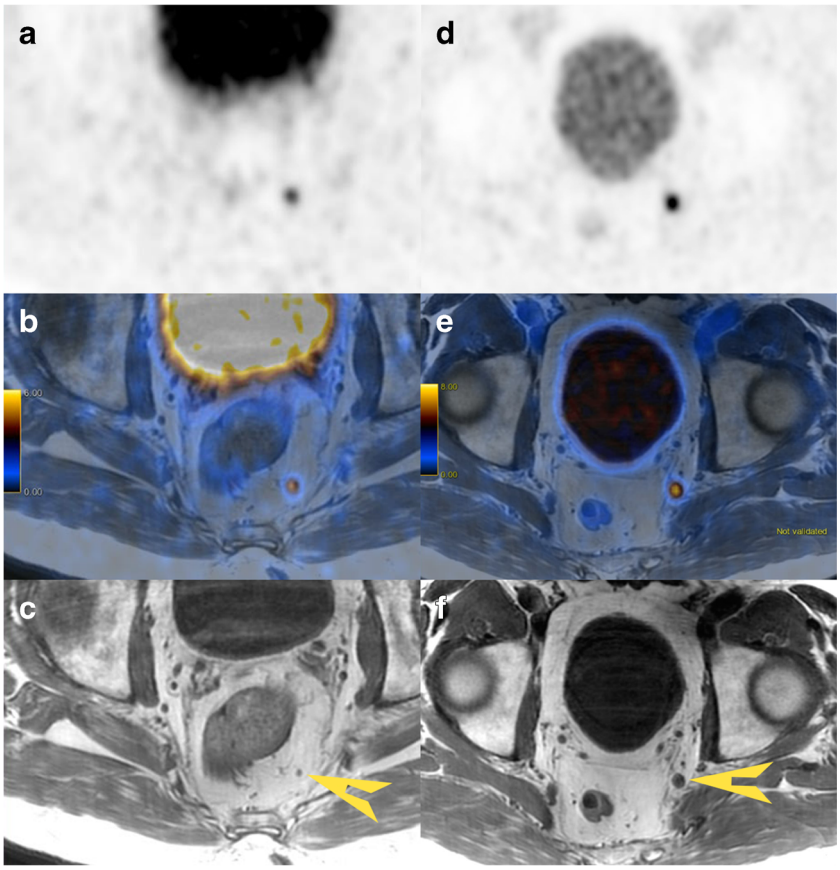

Fig. 4 PSMA-positive lymph node metastases. **a** Axial ^{68}Ga-PSMA-11 PET image in a patient 3 years after radical resection (pT2c, pN0 (0/12), cM0, Pn1, Gleason 4 + 4 = 8), with a current PSA value of 0.22 ng/mL. Focal uptake (SUV_{max}: 6.4) in the left perirectal region, **b** projecting onto a small lesion on fused axial PET/MRI, **c** corresponding to a small (3 mm) lymph node (arrow) on axial T1 weighted image. **d** Axial ^{68}Ga-PSMA-11 PET image in a patient 8 years after resection (pT2c, pN0 (0/23), cM0, Gleason score 3 + 4 = 7, R0) with focal uptake in the left intern iliac region (SUV_{max}: 9.7). **e** Fused PET/MRI images and **f** corresponding 8 mm lymph node (arrow) on axial T1 weighted image

the tracer by using diuretics, early imaging after minutes or very late imaging after 3 h [16, 40]. The optimal time point for imaging is controversial. Early imaging will give the opportunity to image the prostate bed without spill-over from urine activity, while late scans improve the tumor to background ratio. Clear anatomical allocation of tracer activity within the prostate bed, which is feasible with simultaneous PET/MRI, might reduce the interference of urine activity with local recurrence (Fig. 3).

Another, recently reported possibility to reduce artifacts on PET/MRI is the use of TOF information for image reconstruction [22]. The narrowed decay allocation on the line of response due to TOF capacity in PET/MR scanners can improve image resolution and reduce artifacts resulting from incorrect AC [41]. This can especially reduce arm truncation artifacts leading to substantial image artifacts on non TOF PET/MRI [42]. Segmentation for MR-AC is still performed without the incorporation of bone density in most PET/MRI systems. This leads to a systematic underestimation of PET activity around osseous structures [21].

Clinical feasibility for PET/MRI scans is another important fact. With a protocol length of 30 min a median scan time of 42 min with a maximum of 57 min was achieved. Reflecting the fact that some patients needed a toilet break, or there were difficulties with planning the scan.

Other factors such as continued androgen deprivation therapy might also influence the detection rate of ^{68}Ga-PSMA-11 imaging. In vitro data demonstrated an upregulation of PSMA surface receptors by androgen deprivation therapy [43]. In our cohort, only one patient underwent ^{68}Ga-PSMA-11 PET/MRI during androgen-deprivation therapy with ^{68}Ga-PSMA-11 positive lymph nodes at a PSA level of 0.08 ng/mL. Also Afsahr-Oromieh et al. found a significant correlation between ADT at PET scan and pathological findings on PSMA PET/CT [29]. Other, hitherto published studies do not mention if androgen-deprivation was given before imaging.

A limitation of our study is its retrospective nature, leading to an inherent selection bias. Furthermore, the reported patient collective is relatively small and lacks a comparison to another imaging modality (e.g. PET/CT) and histopathology of PSMA-positive lesions. Future investigations are needed to elucidate whether PET/MRI can improve the detection rate of ^{68}Ga-PSMA in patients with early biochemical recurrence and furthermore whether targeted treatment of oligo-metastatic disease improves the cancer-specific survival.

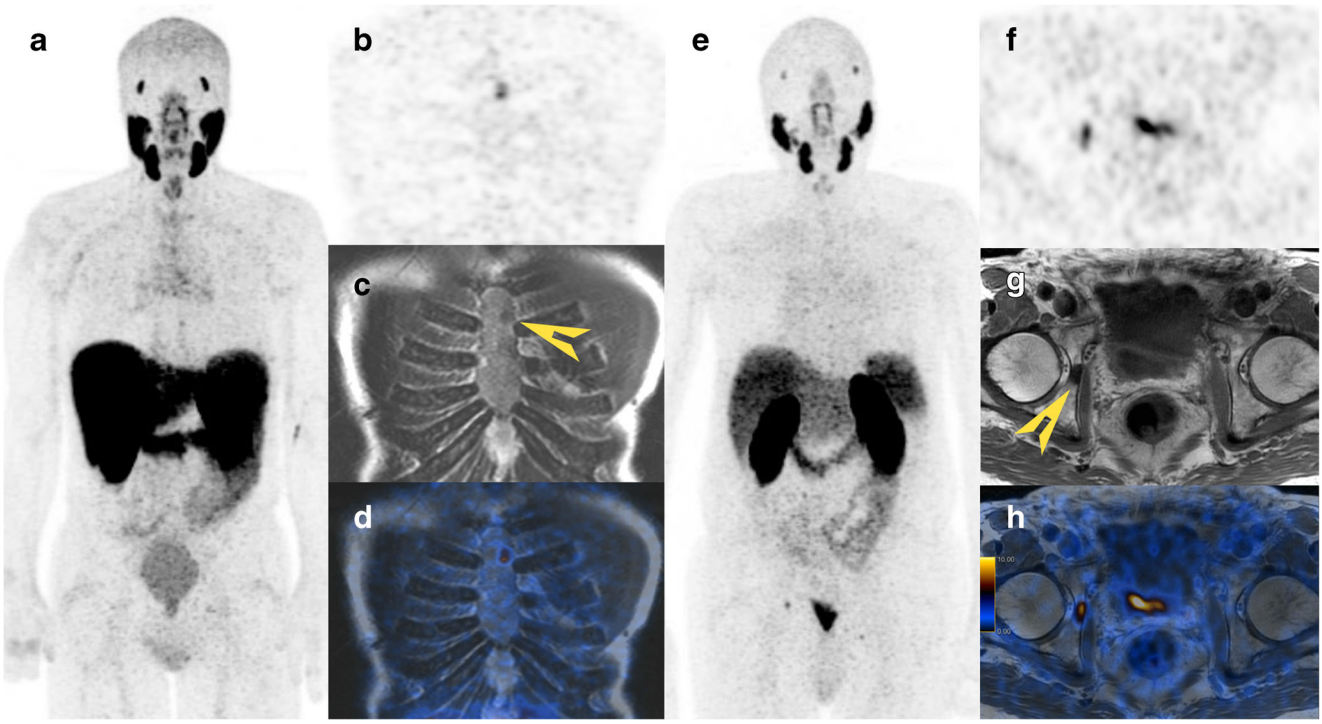

Fig. 5 PSMA-positive bone metastases in patients with low PSA values. **a** MIP ^{68}Ga-PSMA-11 PET of a 65-year-old patient with a solitary 1.1 cm PSMA-positive (SUVmax: 4.1) bone metastasis in the sternum. PSA value at scan 0.14 ng/mL. **b** Coronal PET image with small focal uptake and **c** coronal T2 weighted MRI shows focal hypointensity in the sternum (arrow), **d** correlating well with the increased PSMA uptake. Five months after stereotactic radiotherapy the PSA value dropped to 0.04 ng/ml. Initial tumor stage was pT2c, cN0, cM0, Gleason 3 + 4 = 7, R1. **e/f** MIP and axial ^{68}Ga-PSMA-11 PET with a ^{68}Ga-PSMA-11-positive osseus lesion in the right acetabulum (SUV_{max} 5.9) **g** focal hypointensity on the T1 weighted axial image (arrow), **h** correlating well with the increased PSMA uptake on fused PET/MR images. PSA value at scan 0.96 ng/mL

Conclusion

Our data shows that simultaneous ^{68}Ga-PSMA-11 PET/MRI with TOF has a high detection rate for biochemical recurrence. Furthermore, it shows that even at very low PSA levels <0.5 ng/mL, extrapelvic disease can be localized in 25% of patients with EBR, potentially changing the sRT-planning in a substantial number of patients.

Acknowledgements The authors acknowledge Ms. Sarah Kedzia for the excellent organization of the patient database, and the technicians Marlena Hofbauer, Miguel Porto, Sofia Kaltsuni, Tobias Oblasser and Sabrina Epp for the excellent work on high quality PET/MRI.

Compliance with ethical standards The Department of Nuclear Medicine holds an institutional Research Contract with GE Healthcare. The authors declare that no competing financial interests exist.

This retrospective study was approved by the local ethics committee (BASEC Nr. 2016–02230). All patients gave a written informed general consent for retrospective analysis of their data.

Authors IAB, MH and PAK have received research grants and speaker honorarium from GE Healthcare. Author IAB received research grants from Swiss Life and speaker honorarium from Bayer Health Care and Astellas Pharma AG. Author MG has received research grants from Varian. Authors BK, JM, ASB, PS, DE, HN, UM declare no conflict of interest.

References

1. Torre LA, Bray F, Siegel RL, Ferlay J, Lortet-Tieulent J, Jemal A. Global cancer statistics, 2012. CA Cancer J Clin. 2015;65:87–108. https://doi.org/10.3322/caac.21262.
2. Mottet N, Bellmunt J, Bolla M, Briers E, Cumberbatch MG, De Santis M, et al. EAU-ESTRO-SIOG guidelines on prostate cancer. Part 1: screening, diagnosis, and local treatment with curative intent. Eur Urol. 2016; https://doi.org/10.1016/j.eururo.2016.08.003.
3. Cornford P, Bellmunt J, Bolla M, Briers E, De Santis M, Gross T, et al. EAU-ESTRO-SIOG guidelines on prostate cancer. Part II: treatment of relapsing, metastatic, and castration-resistant prostate cancer. Eur Urol. 2016; https://doi.org/10.1016/j.eururo.2016.08.002.
4. Furubayashi N, Negishi T, Iwai H, Nagase K, Taguchi K, Shimokawa M, et al. Biochemical failure after radical prostatectomy in intermediate-risk group men increases with the number of risk factors. Indian J Urol. 2017;33:64–9. https://doi.org/10.4103/0970-1591.194786.
5. Punnen S, Cooperberg MR, D'Amico AV, Karakiewicz PI, Moul JW, Scher HI, et al. Management of biochemical recurrence after primary treatment of prostate cancer: a systematic review of the literature. Eur Urol. 2013;64:905–15. https://doi.org/10.1016/j.eururo.2013.05.025.
6. Amling CL, Bergstralh EJ, Blute ML, Slezak JM, Zincke H. Defining prostate specific antigen progression after radical prostatectomy: what is the most appropriate cut point? J Urol. 2001;165:1146–51.

7. Pfister D, Bolla M, Briganti A, Carroll P, Cozzarini C, Joniau S, et al. Early salvage radiotherapy following radical prostatectomy. Eur Urol. 2014;65:1034–43. https://doi.org/10.1016/j.eururo.2013.08.013.
8. Tendulkar RD, Agrawal S, Gao T, Efstathiou JA, Pisansky TM, Michalski JM, et al. Contemporary update of a multi-institutional predictive Nomogram for salvage radiotherapy after radical prostatectomy. J Clin Oncol. 2016; https://doi.org/10.1200/JCO.2016.67.9647.
9. Stish BJ, Pisansky TM, Harmsen WS, Davis BJ, Tzou KS, Choo R, et al. Improved metastasis-free and survival outcomes with early salvage radiotherapy in men with detectable prostate-specific antigen after prostatectomy for prostate cancer. J Clin Oncol. 2016; https://doi.org/10.1200/JCO.2016.68.3425.
10. Wiegel T, Lohm G, Bottke D, Hocht S, Miller K, Siegmann A, et al. Achieving an undetectable PSA after radiotherapy for biochemical progression after radical prostatectomy is an independent predictor of biochemical outcome–results of a retrospective study. Int J Radiat Oncol Biol Phys. 2009;73:1009–16. https://doi.org/10.1016/j.ijrobp.2008.06.1922.
11. Robertson NL, Sala E, Benz M, Landa J, Scardino P, Scher HI, et al. Combined whole-body and multi-parametric prostate MRI as a single-step approach for the simultaneous assessment of local recurrence and metastatic disease after radical prostatectomy. J Urol. 2017; https://doi.org/10.1016/j.juro.2017.02.071.
12. Ceci F, Herrmann K, Castellucci P, Graziani T, Bluemel C, Schiavina R, et al. Impact of 11C-choline PET/CT on clinical decision making in recurrent prostate cancer: results from a retrospective two-centre trial. Eur J Nucl Med Mol Imaging. 2014;41:2222–31. https://doi.org/10.1007/s00259-014-2872-x.
13. Giovacchini G, Picchio M, Coradeschi E, Bettinardi V, Gianolli L, Scattoni V, et al. Predictive factors of [(11)C]choline PET/CT in patients with biochemical failure after radical prostatectomy. Eur J Nucl Med Mol Imaging. 2010;37:301–9. https://doi.org/10.1007/s00259-009-1253-3.
14. Afshar-Oromieh A, Avtzi E, Giesel FL, Holland-Letz T, Linhart HG, Eder M, et al. The diagnostic value of PET/CT imaging with the (68)Ga-labelled PSMA ligand HBED-CC in the diagnosis of recurrent prostate cancer. Eur J Nucl Med Mol Imaging. 2015;42:197–209. https://doi.org/10.1007/s00259-014-2949-6.
15. Eiber M, Maurer T, Souvatzoglou M, Beer AJ, Ruffani A, Haller B, et al. Evaluation of hybrid (6)(8)Ga-PSMA Ligand PET/CT in 248 patients with biochemical recurrence after radical prostatectomy. J Nucl Med. 2015;56:668–74. https://doi.org/10.2967/jnumed.115.154153.
16. Kabasakal L, Demirci E, Ocak M, Akyel R, Nematyazar J, Aygun A, et al. Evaluation of PSMA PET/CT imaging using a 68Ga-HBED-CC ligand in patients with prostate cancer and the value of early pelvic imaging. Nucl Med Commun. 2015;36:582–7. https://doi.org/10.1097/MNM.0000000000000290.
17. Einspieler I, Rauscher I, Duwel C, Kronke M, Rischpler C, Habl G, et al. Detection efficacy of hybrid 68Ga-PSMA ligand PET/CT in prostate cancer patients with biochemical recurrence after primary radiation therapy defined by phoenix criteria. J Nucl Med. 2017; https://doi.org/10.2967/jnumed.116.184457.
18. Afshar-Oromieh A, Haberkorn U, Schlemmer HP, Fenchel M, Eder M, Eisenhut M, et al. Comparison of PET/CT and PET/MRI hybrid systems using a 68Ga-labelled PSMA ligand for the diagnosis of recurrent prostate cancer: initial experience. Eur J Nucl Med Mol Imaging. 2014;41:887–97. https://doi.org/10.1007/s00259-013-2660-z.
19. Freitag MT, Radtke JP, Afshar-Oromieh A, Roethke MC, Hadaschik BA, Gleave M, et al. Local recurrence of prostate cancer after radical prostatectomy is at risk to be missed in 68Ga-PSMA-11-PET of PET/CT and PET/MRI: comparison with mpMRI integrated in simultaneous PET/MRI. Eur J Nucl Med Mol Imaging. 2016; https://doi.org/10.1007/s00259-016-3594-z.
20. Eiber M, Weirich G, Holzapfel K, Souvatzoglou M, Haller B, Rauscher I, et al. Simultaneous 68Ga-PSMA HBED-CC PET/MRI improves the localization of primary prostate cancer. Eur Urol. 2016; https://doi.org/10.1016/j.eururo.2015.12.053.
21. Samarin A, Burger C, Wollenweber SD, Crook DW, Burger IA, Schmid DT, et al. PET/MR imaging of bone lesions–implications for PET quantification from imperfect attenuation correction. Eur J Nucl Med Mol Imaging. 2012;39:1154–60. https://doi.org/10.1007/s00259-012-2113-0.
22. Ter Voert EE, Veit-Haibach P, Ahn S, Wiesinger F, Khalighi MM, Levin CS, et al. Clinical evaluation of TOF versus non-TOF on PET artifacts in simultaneous PET/MR: a dual centre experience. Eur J Nucl Med Mol Imaging. 2017; https://doi.org/10.1007/s00259-017-3619-2.
23. Svirydenka H, Delso G, Barbosa FG, Huellner MW, Davison H, Fanti S, et al. The effect of susceptibility artifacts related to metal implants on adjacent lesion assessment in simultaneous TOF PET/MR. J Nucl Med. 2017; https://doi.org/10.2967/jnumed.116.180802.
24. Sekine T, Barbosa FG, Sah BR, Mader CE, Delso G, Burger IA, et al. PET/MR outperforms PET/CT in suspected occult Tumors. Clin Nucl Med. 2017;42:e88–95. https://doi.org/10.1097/RLU.0000000000001461.
25. Hale CA, Fleiss JL. Interval estimation under two study designs for kappa with binary classifications. Biometrics. 1993;49:523–34.
26. Cohen JA. Coefficient of agreement for nominal scales. Educ Psychol Meas. 1960;20:37–46. https://doi.org/10.1177/001316446002000104.
27. Landis JR, Koch GG. The measurement of observer agreement for categorical data. Biometrics. 1977;33:159–74.
28. Freitag MT, Radtke JP, Hadaschik BA, Kopp-Schneider A, Eder M, Kopka K, et al. Comparison of hybrid (68)Ga-PSMA PET/MRI and (68)Ga-PSMA PET/CT in the evaluation of lymph node and bone metastases of prostate cancer. Eur J Nucl Med Mol Imaging. 2016;43:70–83. https://doi.org/10.1007/s00259-015-3206-3.
29. Afshar-Oromieh A, Holland-Letz T, Giesel FL, Kratochwil C, Mier W, Haufe S, et al. Diagnostic performance of 68Ga-PSMA-11 (HBED-CC) PET/CT in patients with recurrent prostate cancer: evaluation in 1007 patients. Eur J Nucl Med Mol Imaging. 2017;44:1258–68. https://doi.org/10.1007/s00259-017-3711-7.
30. Fendler WP, Calais J, Allen-Auerbach M, Bluemel C, Eberhardt N, Emmett L, et al. 68Ga-PSMA-11 PET/CT interobserver agreement for prostate cancer assessments: an international multicenter prospective study. J Nucl Med. 2017; https://doi.org/10.2967/jnumed.117.190827.
31. Schiller K, Sauter K, Dewes S, Eiber M, Maurer T, Gschwend J, et al. Patterns of failure after radical prostatectomy in prostate cancer - implications for radiation therapy planning after 68Ga-PSMA-PET imaging. Eur J Nucl Med Mol Imaging. 2017; https://doi.org/10.1007/s00259-017-3746-9.
32. Verburg FA, Pfister D, Heidenreich A, Vogg A, Drude NI, Voo S, et al. Extent of disease in recurrent prostate cancer determined by [(68)Ga]PSMA-HBED-CC PET/CT in relation to PSA levels, PSA doubling time and Gleason score. Eur J Nucl Med Mol Imaging. 2016;43:397–403. https://doi.org/10.1007/s00259-015-3240-1.
33. Kabasakal L, Demirci E, Nematyazar J, Akyel R, Razavi B, Ocak M, et al. The role of PSMA PET/CT imaging in restaging of prostate cancer patients with low prostate-specific antigen levels. Nucl Med Commun. 2016; https://doi.org/10.1097/MNM.0000000000000617.
34. Afshar-Oromieh A, Zechmann CM, Malcher A, Eder M, Eisenhut M, Linhart HG, et al. Comparison of PET imaging with a (68)Ga-labelled PSMA ligand and (18)F-choline-based PET/CT for the diagnosis of recurrent prostate cancer. Eur J Nucl Med Mol

Imaging. 2014;41:11–20. https://doi.org/10.1007/s00259-013-2525-5.
35. Pfob CH, Ziegler S, Graner FP, Kohner M, Schachoff S, Blechert B, et al. Biodistribution and radiation dosimetry of (68)Ga-PSMA HBED CC-a PSMA specific probe for PET imaging of prostate cancer. Eur J Nucl Med Mol Imaging. 2016;43:1962–70. https://doi.org/10.1007/s00259-016-3424-3.
36. Afshar-Oromieh A, Hetzheim H, Kubler W, Kratochwil C, Giesel FL, Hope TA, et al. Radiation dosimetry of (68)Ga-PSMA-11 (HBED-CC) and preliminary evaluation of optimal imaging timing. Eur J Nucl Med Mol Imaging. 2016;43:1611–20. https://doi.org/10.1007/s00259-016-3419-0.
37. Uprimny C, Kroiss AS, Decristoforo C, Fritz J, Warwitz B, Scarpa L, et al. Early dynamic imaging in 68Ga- PSMA-11 PET/CT allows discrimination of urinary bladder activity and prostate cancer lesions. Eur J Nucl Med Mol Imaging. 2017;44:765–75. https://doi.org/10.1007/s00259-016-3578-z.
38. Noto B, Buther F, Auf der Springe K, Avramovic N, Heindel W, Schafers M, et al. Impact of PET acquisition durations on image quality and lesion detectability in whole-body 68Ga-PSMA PET-MRI. EJNMMI Res. 2017;7:12. https://doi.org/10.1186/s13550-017-0261-8.
39. Lutje S, Blex S, Gomez B, Schaarschmidt BM, Umutlu L, Forsting M, et al. Optimization of acquisition time of 68Ga-PSMA-Ligand PET/MRI in patients with local and metastatic prostate cancer. PLoS One. 2016;11:e0164392. https://doi.org/10.1371/journal.pone.0164392.
40. Derlin T, Weiberg D, von Klot C, Wester HJ, Henkenberens C, Ross TL, et al. 68Ga-PSMA I&T PET/CT for assessment of prostate cancer: evaluation of image quality after forced diuresis and delayed imaging. Eur Radiol. 2016;26:4345–53. https://doi.org/10.1007/s00330-016-4308-4.
41. Mehranian A, Arabi H, Zaidi H. Vision 20/20: magnetic resonance imaging-guided attenuation correction in PET/MRI: challenges, solutions, and opportunities. Med Phys. 2016;43:1130–55. https://doi.org/10.1118/1.4941014.
42. Afshar-Oromieh A, Wolf M, Haberkorn U, Kachelriess M, Gnirs R, Kopka K, et al. Effects of arm truncation on the appearance of the halo artifact in 68Ga-PSMA-11 (HBED-CC) PET/MRI. Eur J Nucl Med Mol Imaging. 2017; https://doi.org/10.1007/s00259-017-3718-0.
43. Wright GL Jr, Grob BM, Haley C, Grossman K, Newhall K, Petrylak D, et al. Upregulation of prostate-specific membrane antigen after androgen-deprivation therapy. Urology. 1996;48:326–34.